BIOLOGY OF REPRODUCTION (2015) **92**(2):37, 1–11
Published online before print 17 December 2014.
DOI 10.1095/biolreprod.114.126326

Processive Pulses of Retinoic Acid Propel Asynchronous and Continuous Murine Sperm Production[1]

Cathryn A. Hogarth,[3] Samuel Arnold,[4] Travis Kent,[3] Debra Mitchell,[3] Nina Isoherranen,[4] and Michael D. Griswold[2,3]

[3]*School of Molecular Biosciences and the Center for Reproductive Biology, Washington State University, Pullman, Washington*
[4]*University of Washington Medical Center, University of Washington, Seattle, Washington*

ABSTRACT

The asynchronous cyclic nature of spermatogenesis is essential for continual sperm production and is one of the hallmarks of mammalian male fertility. While various mRNA and protein localization studies have indirectly implicated changing retinoid levels along testis tubules, no quantitative evidence for these changes across the cycle of the seminiferous epithelium currently exists. This study utilized a unique mouse model of induced synchronous spermatogenesis, localization of the retinoid-signaling marker STRA8, and sensitive quantification of retinoic acid concentrations to determine whether there are fluctuations in retinoid levels at each of the individual stages of germ cell differentiation and maturation to sperm. These data show that processive pulses of retinoic acid are generated during spermatogonial differentiation and are the likely trigger for cyclic spermatogenesis and allow us, for the first time, to understand how the cycle of the seminiferous epithelium is generated and maintained. In addition, this study represents the first direct quantification of a retinoid gradient controlling cellular differentiation in a postnatal tissue.

retinoic acid, spermatogenesis, spermatogonia, testis

INTRODUCTION

Small molecule morphogen gradients are believed to direct cell fate decisions via localized changes in concentrations. Based largely on qualitative transcript localization studies, gradients of retinoic acid (RA), the active metabolite of vitamin A, are predicted to be essential for patterning various embryonic tissues and organs [1–6]. While indirect visualization of embryonic RA gradients in zebrafish has just recently been achieved [7], direct and quantitative measurements of these gradients have been hindered by low RA concentrations and limited tissue availability. In addition, even though more and more evidence indicates a critical role for RA in the proper function of many mammalian postnatal organ systems [8–14], no studies have directly demonstrated that retinoid gradients exist following birth.

One of the postnatal tissues requiring RA is the testis. It has been known since 1925 that vitamin A is required for male fertility, yet the specifics of how RA levels are regulated within the testis, the cell types under RA control, and the downstream mechanisms triggered by RA signaling are still being elucidated. Based solely on mRNA and protein localization patterns, recent studies have postulated that specific expression of the RA storage, synthesis, and degradation enzymes result in gradients or pulses of RA within testis tubules [8, 15–17]. These observations have led to the concept that endogenous RA pulses drive the periodic differentiation of male germ cells and, as a result, are the trigger for continual sperm production [8, 17, 18] (Fig. 1). This hypothesis is also supported by the detection of RA activity via the visualization of a reporter gene under the transcriptional control of a RA response element in the neonatal testis [19]. Snyder et al. [19] demonstrated that RA activity occurs within discrete patches along the length of neonatal testis tubules, implying that RA is generated only within these patches at the onset of spermatogenesis. These patches are the first evidence for the establishment of numerous RA gradients that lead to asynchronous sperm production. In addition, the localization of the classic marker of germ cell response to RA, stimulated by retinoic acid gene 8 (STRA8), to these patches and to specific cell types within distinct tubules of the adult testis also supports the RA pulse hypothesis [18–20]. However, these predicted oscillations in testicular RA levels have yet to be visualized or quantitatively measured in the postnatal testis, due mostly to the complex nature of how the developing germ cells are arranged within this organ. In fact, utilizing mRNA localization data, Sugimoto et al. [17] proposed a model to describe how RA levels peak at specific points along testis tubules but noted that technical limitations and the complexity of the postnatal testis prevented the measurement of oscillating RA levels and direct testing of their model.

Testis tubules contain different layers of developing germ cells, with cells at very specific points in their differentiation pathway always found in association, termed stages [21] (Fig. 1). These stages reappear at any single point along a tubule in a cyclic manner and are arranged sequentially along the tubule in what has been defined as the spermatogenic wave [21]. The sequential arrangement of recurring stages guarantees continuous and asynchronous sperm production characteristic of fertile male mammals, yet this complex arrangement makes it nearly impossible to examine different sections of tubules in

[1]This work was supported by NIH grants R01 10808 to M.D.G., U54 HD42454 to M.D.G. and N.I., and R01 GM111772 to N.I. and C.A.H. This project was also partially supported by Award number T32 GM083864 to T.K. from the NIGMS and TL1 TR000422 to S.A. from the NCATS. The content is solely the responsibility of the authors and does not necessarily represent the official views of the NIH. Presented in part at the 47th Annual Meeting of the Society for the Study of Reproduction, 19–23 July, Grand Rapids, Michigan. The NCBI GEO accession number for the microarray analysis performed in this study is GSE64214.
[2]Correspondence: Michael Griswold, School of Molecular Biosciences, PO Box 647520, Washington State University, Pullman, WA 99164. E-mail: mgriswold@vetmed.wsu.edu

Received: 30 October 2014.
First decision: 26 November 2014.
Accepted: 9 December 2014.

eISSN: 1529-7268 http://www.biolreprod.org
ISSN: 0006-3363

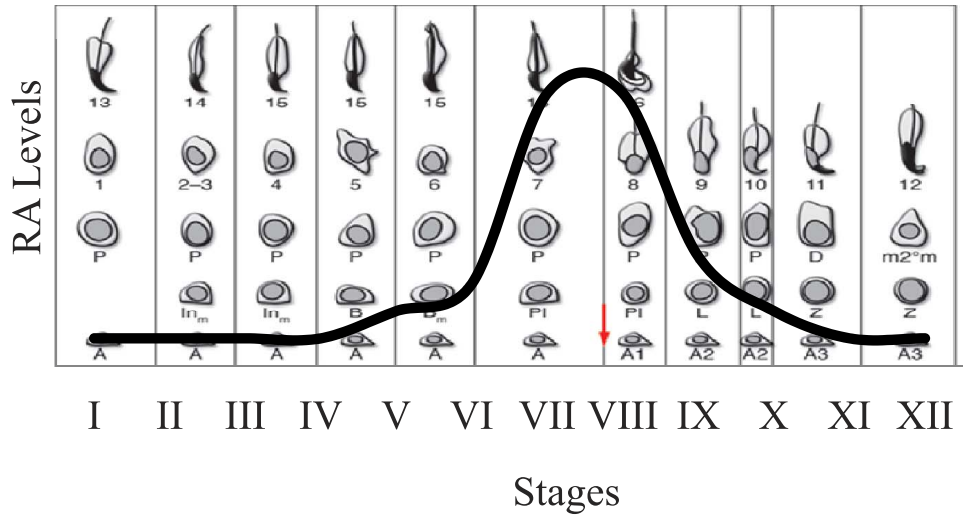

FIG. 1. The RA pulse hypothesis. Various in situ hybridization and immunohistochemistry experiments have led us and others to propose a model whereby retinoid storage, synthesis, and/or degradation is regulated such that RA levels are lowest during Stages II–VI and peak at Stage VIII of the cycle of the seminiferous epithelium during testis development. Processes known to be regulated by RA, including spermatogonial differentiation, spermiation, and blood-testis barrier reorganization, all take place during Stage VIII, and there is currently no known role for RA during Stages II–VI.

isolation within a wild-type testis. We recently developed a method using bisdichloroacetyldiamine (WIN 18,446) and RA to synchronize spermatogenesis in both juvenile and adult testes [22] as a means of overcoming this complexity. WIN 18,446 is a potent inhibitor of the retinaldehyde dehydrogenases (RALDHs) [23], the enzymes responsible for oxidizing retinaldehyde to RA, and treatment of male mice with this compound results in a decrease in intratesticular RA levels, blocking male germ cell differentiation and generating testes full of undifferentiated type A spermatogonia [22, 23]. Following WIN 18,446 treatment with an injection of RA, spermatogonia begin to differentiate simultaneously, driving synchronous spermatogenesis. As a result, while the cycling of the stages is unaffected, the sequential arrangement of the stages along the tubule is eliminated. This treatment results in the creation of juvenile testes full of germ cells undergoing the same differentiation step or adult mouse testes containing tubules with the same germ cell composition (only two to three stages) throughout the entire testis [22]. This methodology allows for the accurate assessment of individual processes or measurement of morphogens within the testis by dramatically increasing the homogeneity of cells or stages present during the different steps of spermatogenesis.

To investigate whether there are measurable pulses of RA within the postnatal testis and to further characterize the localization and function of STRA8, we utilized our WIN 18,446/RA protocol combined with a highly sensitive liquid chromatography/tandem mass spectroscopy assay to quantitate changes in retinoid levels and localize STRA8 protein in testis samples collected from animals with synchronized spermatogenesis and in those where wild-type RA levels had been altered. Interestingly, we have measured, for the first time, pulses of RA occurring during Stage VIII and IX of the seminiferous cycle, aligning perfectly with the onset of STRA8 expression in spermatogonia and spermatocytes at these stages. These data indicate that the presence or absence of STRA8 protein within germ cells is highly dependent on the availability of RA within the seminiferous epithelium. In addition, this study represents the first direct quantification of a retinoid gradient controlling cellular differentiation in a postnatal tissue.

MATERIALS AND METHODS

Animals and Tissues

All the animal experiments were approved by the Washington State University Animal Care and Use Committees and were conducted in accordance with the guiding principles for the care and use of research animals of the National Institutes of Health. All the experiments were performed with mixed background C57BL/6 × 129 mice housed in a temperature- and humidity-controlled environment with food and water provided ad libitum. The animals were euthanized by CO_2 asphyxiation followed by decapitation (0–10 days postparturition [dpp]) or cervical dissociation (10 dpp to adult) and their testes dissected. Samples for RA measurements were snap frozen immediately after collection in a light-protected tube and stored at −80°C until use. Testis samples for morphological and immunohistochemical analyses were fixed in Bouin fixative for between 2 and 8 h, depending on sample size, and then dehydrated through a graded ethanol series before being embedded in paraffin wax. Sections of 4 μm were placed on Superfrost Plus slides (Menzel-Glaser).

WIN 18,446 and RA Treatments

Spermatogenesis was synchronized using the following protocol [22]: 2 dpp mice were pipette fed 100 μg/g body weight WIN 18,446, suspended in 1% gum tragacanth, for 7 consecutive days. On 9 dpp (Day 8 of treatment), the testes from some animals were collected as the time zero samples (WIN 18,446 or vehicle control only-treated animals) and the rest were given either a subcutaneous injection of 200 μg of RA (Sigma-Aldrich) in 10 μl of dimethyl sulfoxide (DMSO) (WIN 18,446-treated animals) or 10 μl DMSO alone (vehicle control only-treated animals), and then left to recover for various intervals between 1 and 16 days postinjection. Three pooled samples, each weighing at least 150 mg, were collected for the control and treated groups at each time point. As the amount of tissue needed to accurately perform the RA quantification was more than the weight of testes from one neonatal animal for most time points, testes were pooled until the required weight was reached. This varied from 15–18 animals required for the 0 and 1 day postinjection samples to only one to two animals needed for the 16 days postinjection samples. To induce synchronous spermatogenesis in the adult testis, the same WIN 18,446/RA treatment regimen (described above) was utilized, however, these animals were left to recover for various intervals between 42 and 50 days postinjection. Control animals received 1% gum tragacanth plus an injection of 10 μl DMSO. For the exogenous RA experiments, vitamin A-sufficient adult male mice (n = 3 for both vehicle control and treated groups) were treated with a single dose of 0.5 mg RA, in 100 μl 15% DMSO/85% sesame oil, via intraperitoneal injection. The testes were collected from these animals 24 h following treatment and fixed for morphology analysis and STRA8 immunohistochemistry. Control animals received a single injection of only 100 μl 15% DMSO/85% sesame oil.

Adult Mouse Testis Staging

Tubule cross-sections from all adult mouse testis samples, both wild type and synchronized, were staged according to the criteria described by Russell et al. [21]. More specifically, the development of the acrosome and elongating spermatid cytoplasmic shape and positioning within the seminiferous epithelium were predominantly used for Stages I–VI, that is, elongating spermatids at Stage II–III contain more cytoplasm and are positioned closer to the lumen of the tubule whereas at Stage V, elongating spermatids contain less cytoplasm and the head of the spermatid is positioned closer to the basement membrane. Stage VII and Stage VIII tubules were differentiated by the position of the nucleus within the round spermatids, numbers of preleptotene spermatocytes (these cells first appear at Stage VII but many more are present Stage VIII), and by the connection of the step 16-elongating spermatids to the seminiferous epithelium. Stages IX, X, and XI were differentiated by the shape of the elongated spermatid (both of the nucleus and the cytoplasm) and of the size and shape of the pachytene and/or presence of diplotene spermatocytes. Finally, Stage XII was defined by the presence of spermatocytes containing condensed chromosomes at either metaphase, anaphase, or telophase.

Analysis of Synchronized Tissue

For the adult testis RA measurements, a minimum of 200 testis cross-sections on a minimum of two planes separated by a minimum of 50 μm from each of the 10 vehicle control-treated samples or 26 WIN 18,446/RA-treated samples were assigned as displaying a particular stage of the seminiferous epithelium based on the criteria described above [21]. The midpoint of synchrony, window width, and synchrony factor for each of the 26 WIN 18,446/RA-treated adult synchronized samples was calculated following the methods described by Van Beek and Meistrich [24] and Siiteri et al. [25], and samples displaying a synchrony factor of less than three were then discarded from the analysis, reducing the number of WIN 18,446/RA-treated samples from 26 to 20. The window width provides information regarding which stages are represented within samples and allows for qualitative assessments of the effect of the presence of different stages on RA levels within individual samples [24, 25]. The synchrony factor is a numerical representation of the comparison between the control and synchronized samples and is calculated by dividing the window width of the control samples by the window width of the synchronized samples [24, 25]. The midpoint of synchrony provides a reference point within each window width to demonstrate at which point along the cycle that sample is synchronized and is the most accurate way of analyzing differences between synchronized testis samples because the calculation takes into consideration the time it takes to progress from one stage to the next [24, 25].

Immunohistochemistry

We generated a rabbit polyclonal antibody raised against recombinant full-length STRA8 protein. Immunohistochemistry using the collected STRA8 antisera was performed essentially as previously described [26]. Antigen retrieval was performed in 0.01 M citrate (pH 6 and >90°C maintained for 5 min), and STRA8 antisera was applied at a dilution of 1:2000 for overnight incubation at room temperature in 5% normal goat serum, 0.1% bovine serum albumin, and PBS (137 mM NaCl, 2.7 mM KCl, 10.1 mM Na_2HPO_4, and 1.8 mM KH_2PO_4). Control sections were incubated with preimmune serum. Subsequent steps were performed at room temperature, with PBS washes between incubations. Primary antibody binding was detected using the ready-to-use biotinylated goat anti-rabbit antibody Histostain kit (Invitrogen) conjugated to horseradish peroxidase using the Vectastain Elite ABC kit (Vector Laboratories) according to the manufacturer's instructions. Antibody binding was detected as a brown precipitate following development with 3,3′-diaminobenzidine tetrahydrochloride (Sigma-Aldrich). The sections were mounted under glass coverslips in DPX (VWR International). Germ and somatic cell types were identified on the basis of their nuclear morphology and position within the developing gonad, and the stages of the seminiferous epithelium were identified based on the descriptions in Russell et al. [21]. Sections from at least three C57BL/6 × 129 animals were analyzed for protein localization, and each immunohistochemistry or immunofluorescence experiment was repeated with consistent results obtained. For the vitamin A-sufficient animals injected with RA, STRA8-positive spermatogonia were identified based on nuclear morphology and position within the seminiferous epithelium clearly made visible by the brown staining within either the cytoplasm and/or the nucleus following immunohistochemistry. These cells were quantified by counting the number of positive cells per stage in a minimum of 200 testis cross-sections on a minimum of two planes separated by a minimum of 50 μm from each of the six samples. The ratio of this value for each treatment compared to that of the vehicle control was then used for all statistical analyses. A Student *t*-test (Microsoft Excel) was performed to determine statistically significant differences between vehicle and treated samples. In all cases, a minimum of three biological replicates and technical duplicates were utilized for analysis.

Microarray Analysis

Ten male mice were treated with the WIN 18,446/RA protocol (described above) and left to recover for between 42 and 50 days post-RA injection. Testes were then collected, one testis was fixed in Bouin fixative for morphology analysis, and the second snap frozen on dry ice for RNA extraction. Samples were assigned to one of five different specific groups (n = 2 samples per group) based on the stages represented by that sample. RNA from each sample was extracted using TRI-ZOL (Invitrogen) and run on Affymetrix GeneChip Mouse Gene 1.0 ST microarrays (Aligent Technologies). Array output was normalized via the GC robust multiarray method and data and statistical analysis was conducted using GeneSpring version 12.6.1 (Agilent Technologies). Genes were considered stage-specific during synchronized spermatogenesis if they: 1) had a raw score of greater than 50 in at least one sample, 2) were determined to be significantly different versus at least two other groups by ANOVA ($P = 0.05$) with a 5% false discovery rate multiple test correction, and 3) showed a 2-fold or greater increase or decrease versus at least two other groups. Data was deposited with the National Center for Biotechnology Information gene expression and hybridization array data repository (GEO, http://www.ncbi.nlm.nih.gov/geo) and was assigned the accession number GSE64214.

RA Measurements

The concentration of *all-trans*-RA was measured using an AB Sciex 5500 qTrap Q-LIT mass spectrometer equipped with an Agilent 1290 UHPLC as previously described [27] with several minor modifications. Mouse tissue was homogenized in a 1:1 volume of 0.9% NaCl, a 2:1 volume of acetonitrile (ACN) with 1% formic acid and 10 μl of 1 μM *all-trans*-RA-d_5 (internal standard) was added, and RA was extracted with 10 ml of hexane. The organic layer was dried under nitrogen, and the sample reconstituted in 60:40 ACN/water. The *all-trans*-RA and 13-*cis*-RA were separated using a 150 mm × 2.1 mm Supelco Ascentis Express reverse phase amide column (Sigma) with 2.7 μm particle size with Ascentis Express reverse phase amide guard cartridge and mobile phase consisting of water + 0.1% formic acid (A) and ACN/methanol (60/40) + 0.1% formic acid (B). The solvent flow was 500 μl/min, and the following linear gradient was used: 0.0–2.0 min 40% B, then increased to 95% B at 10.0 min, 10.0–15.0 min 95% B, and then 15.0–17.0 min 40% B. The *all-trans*-RA and was detected using positive ion atmospheric pressure chemical ionization and mass spectral transitions of mass-to-charge ratio (*m*/*z*) of 301–205 and *m*/*z* 301–123 with the 205 fragment used for quantification. For quantification, the *all-trans*-RA and 13-*cis*-RA peak areas were normalized to the *all-trans*-RA-d_5 internal standard area.

RESULTS

STRA8 Displays Stage- and Intracellular-Specific Localization Patterns in the Adult Wild-Type Testis

Previous publications have demonstrated that *Stra8* mRNA displays a stage-specific expression pattern in the adult mouse testis, but this has yet to be fully examined at the protein level [20]. To further investigate this, we generated an antibody raised against full-length recombinant STRA8 protein and performed immunohistochemistry on sections of adult mouse testes (Fig. 2). Consistent with previous observations [18, 20], spermatogonia and preleptotene and leptotene spermatocytes were positive for STRA8 protein in the adult mouse testis but in a tubule-specific manner (Fig. 2). STRA8-positive cells were never present in every tubule throughout an entire cross-section in any sample tested. A stage-specific STRA8 localization pattern was present, with a switch occurring between Stages VII and VIII (Fig. 2, G and H). At Stages V, VI, and VII, no STRA8 was detectable in any cell type (Fig. 2E–G) yet at Stage VIII, differentiating A1 spermatogonia and preleptotene spermatocytes were clearly positive for this protein (Fig. 2H). Signal was detected in differentiating A1-4 spermatogonia in Stages I, IX, X, XI, XII (Fig. 2, C and I–L), and in some

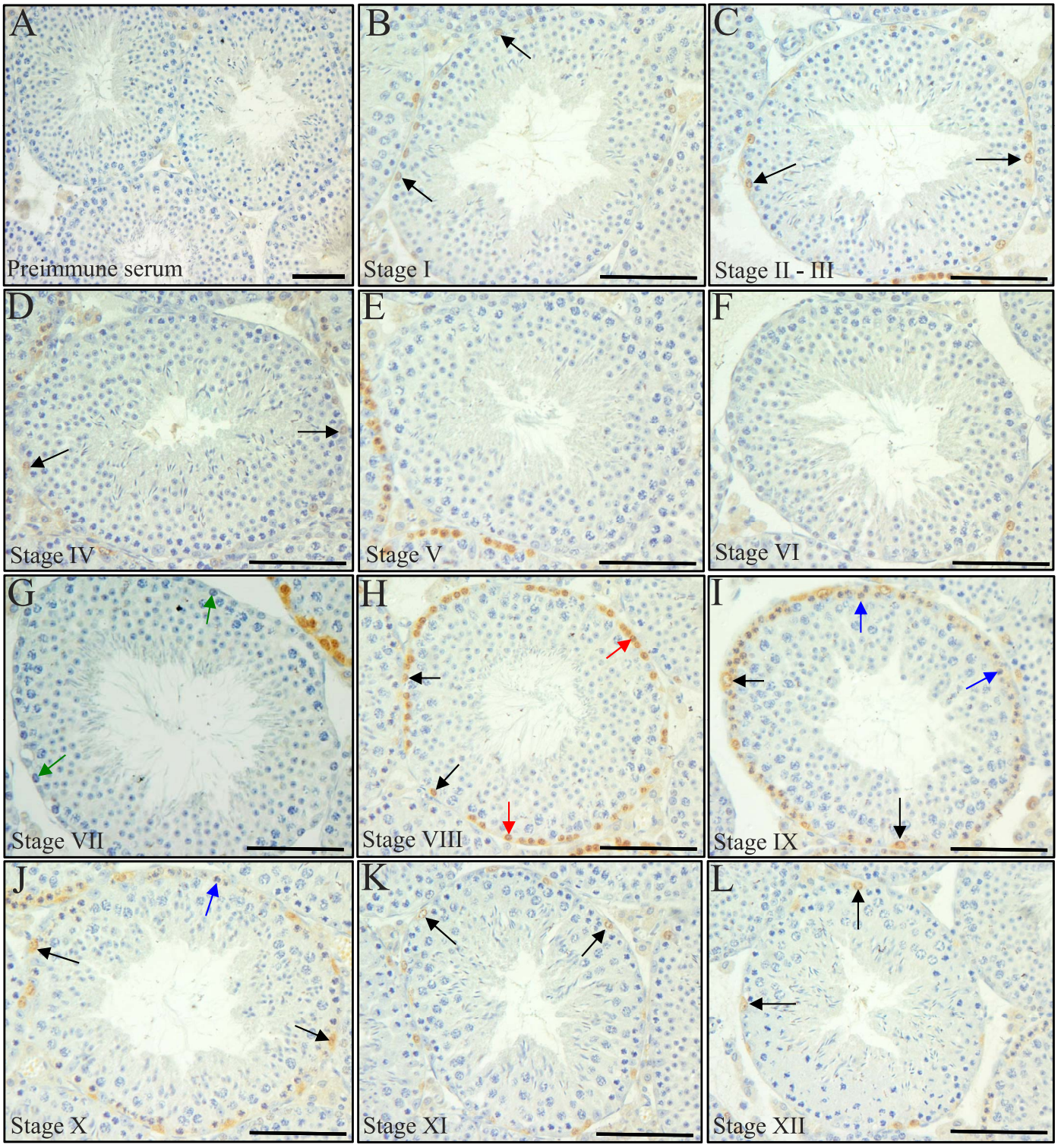

FIG. 2. STRA8 displays a stage-specific localization pattern. **A–L**) Pictures depict STRA8 localization in every stage of the cycle of the seminiferous epithelium in a wild-type adult mouse testis. Black arrows denote STRA8-positive spermatogonia, red arrows denote STRA8-positive preleptotene spermatocytes, green arrows denote STRA8-negative preleptotene spermatocytes in Stage VII, and blue arrows denote STRA8-positive leptotene spermatocytes. Control sections were incubated with preimmune serum (**A**). Bars = 50 μm.

intermediate spermatogonia at Stages II–III and IV (Fig. 2, C and D). Leptotene spermatocytes were also faintly positive for STRA8 protein at Stages IX and X (Fig. 2, I and J). In addition, examination of STRA8 within spermatogonia revealed an interesting stage-specific switch in subcellular localization pattern for this protein. STRA8 was detected in both the cytoplasm and nucleus of A1 or A2 spermatogonia at Stage IX–XI but switched to be predominantly present only in the nucleus as these cells differentiated to A4 spermatogonia at Stage II–III (Fig. 3, A–D).

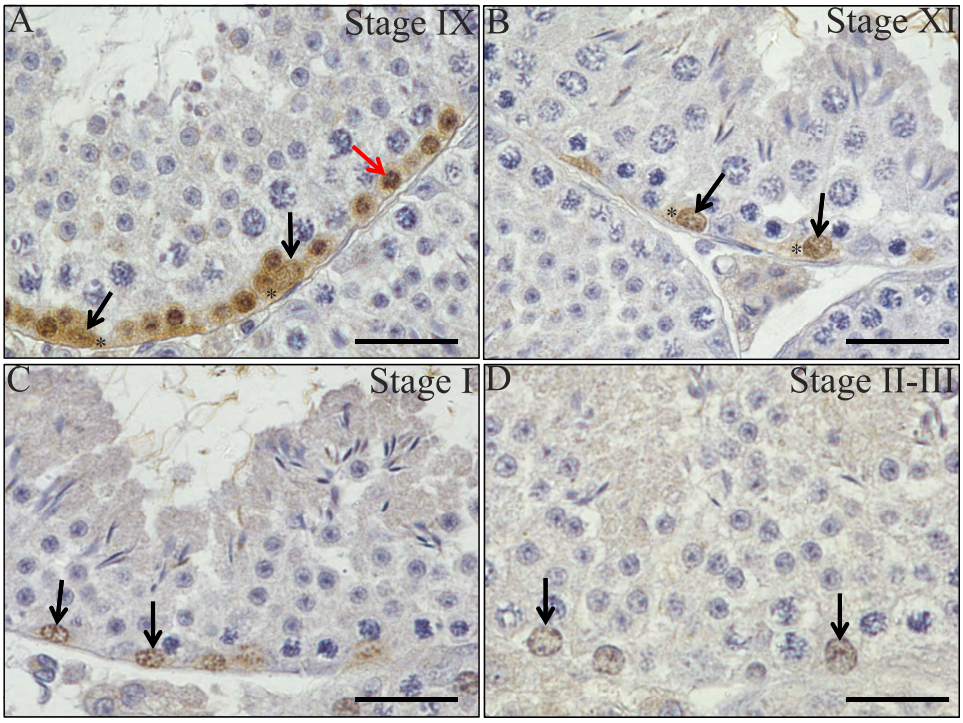

FIG. 3. STRA8 displays cell type-specific intracellular localization patterns in the testis. **A**–**D**) Pictures depict STRA8 localization in Stages IX (**A**), XI (**B**), I (**C**), and II–III (**D**) of the cycle of the seminiferous epithelium in a wild-type adult mouse testis. Black arrows denote STRA8-positive nuclei, and asterisks denote STRA8-positive cytoplasm within spermatogonia. The red arrow highlights a STRA8-positive nucleus within a preleptotene spermatocyte. Bars = 20 μm.

Exogenous RA Only Alters STRA8 Expression in Stages II–VI of the Vitamin A-Sufficient Testis

The stage-specific expression of STRA8 protein strongly supports the hypothesis that RA is only available to germ cells in distinct segments along testis tubules. To investigate this, we injected vitamin A-sufficient adult male mice with RA to determine whether there were specific stages of the cycle that were more susceptible to exogenous RA treatment. No difference was seen in either the intracellular or stage-specific localization pattern of STRA8 in the vehicle control animals when compared to untreated wild-type samples. In contrast, 24 h following treatment of male mice with a single dose of exogenous RA, ectopic expression of STRA8 was induced within spermatogonia, but only within Stages II–VII (Fig. 4, A and B). Cell counts comparing control with RA-treated animals revealed that a significant increase in the number of STRA8-positive spermatogonia per tubule was seen in both Stages II–VI and VII–VIII, and not in the other two stages (Fig. 4D). The increase in the numbers of STRA8-positive spermatogonia in Stages VII–VIII was contributed mostly by ectopic expression of STRA8 in spermatogonia present in Stage VII.

Cyclic Changes in Retinoid-Metabolizing Enzymes Can Be Detected in the Synchronized Testis

To further investigate how RA levels are regulated across the cycle of the seminiferous epithelium, we performed a microarray analysis on testis samples with WIN 18,446/RA-induced synchronized spermatogenesis to examine retinoid-metabolizing enzyme gene expression across the stages. Consistent with the localization studies, *Lrat* transcript was found at significantly lower levels (>2-fold, $P < 0.05$) in Stages VIII–IX when compared to Stages IV–VI (Fig. 5A). However, in contrast to previous localization studies [16, 17], ANOVA comparison of the six distinct groups of synchronized samples revealed no statistically significant fold changes for any of the *Raldh* (Fig. 5B) or *Cyp26* mRNAs (Fig. 5C). Transcripts known to be stage-specific across the cycle—*Stra8* [20, 28], androgen receptor (*Ar*), [29], galectin1 (*Lgals1*) [17], and cathespin L (*Ctsl*) [28]—displayed statistically significant trends consistent with previous studies (Fig. 5D), indicating that the lack of stage-specificity seen for *Raldh* or *Cyp26* was not due to an issue with the samples. Interestingly, statistically significant stage-specific expression ($P < 0.05$) was present for cellular retinoic acid binding protein 1 (*Crabp1*) and for retinol dehydrogenase 10 (*Rdh10*) and dehydrogenase/reductase (SDR family) member 4 (*Dhrs4*), two of the enzymes that regulate the reversible conversion of retinol to retinaldehyde (Fig. 5A).

RA Levels Are Highest Within the Testis when STRA8 Protein Is Present During the First Wave of Spermatogenesis

With a more complete picture of the localization pattern of STRA8 in place and quantitative gene expression evidence to suggest that RA availability changes across the cycle, RA levels in tubules that either contained or were devoid of STRA8 protein were next quantified. To first determine whether pulses of RA could be detected within the juvenile testis, neonatal male mice were treated with our WIN 18,446/RA protocol or vehicle control and then left to recover for various intervals spanning the first two waves of spermatogonial differentiation in the synchronized juvenile testis (Fig. 6). Comparison of RA levels at zero time (24 h following the last WIN 18,446 treatment) in vehicle control and treated animals confirmed that WIN 18,446 was able to significantly lower intratesticular RA levels (Fig. 6A, zero time), indicating that RA synthesis had been successfully inhibited within these

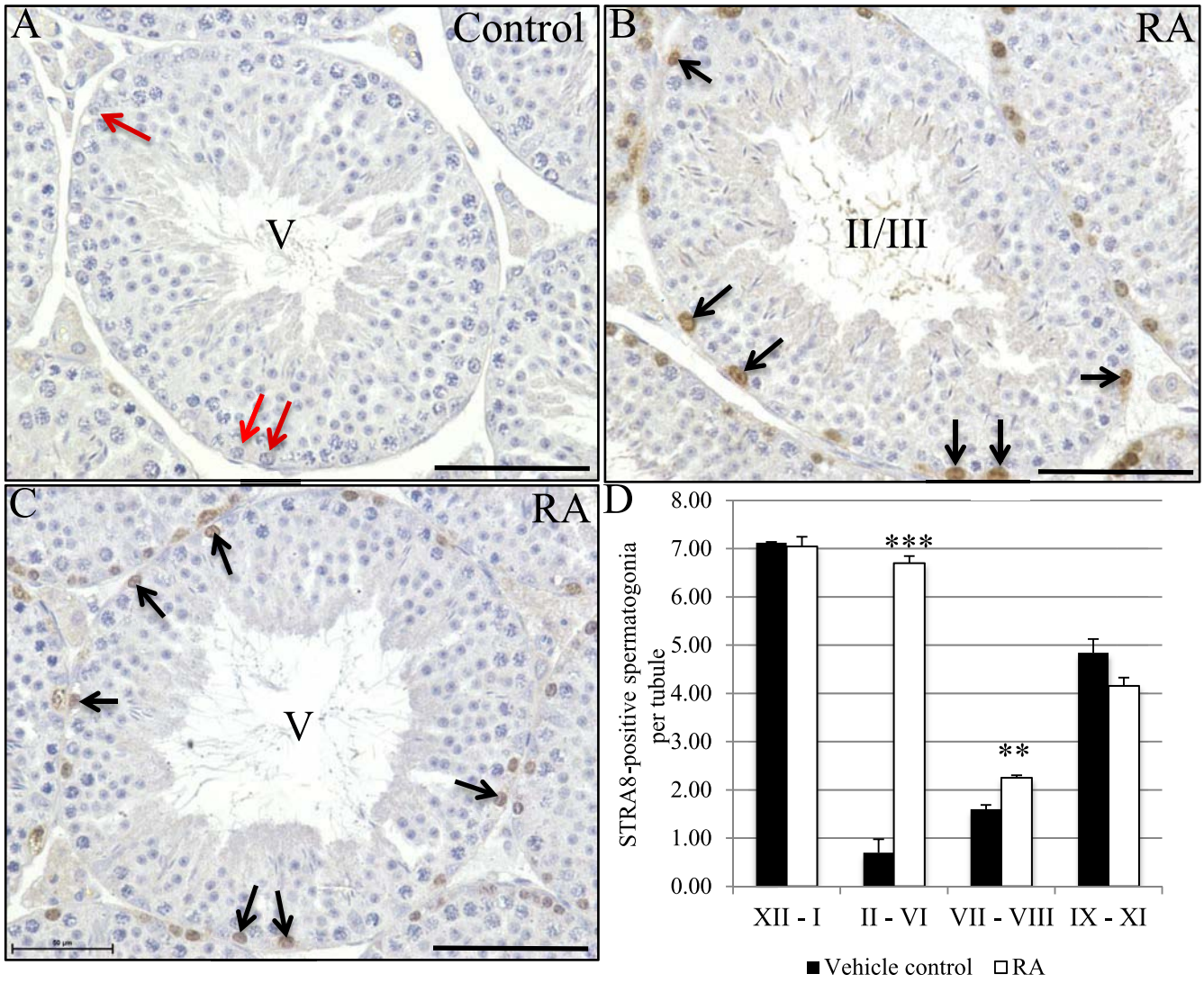

FIG. 4. Stages II–VI are the most susceptible to exogenous RA treatment. **A**–**C**) Pictures depicting STRA8 localization in Stages II–VI in vehicle control (**A**) and RA-treated (**B**, **C**) vitamin A-sufficient adult male mice. Black arrows denote STRA8-positive spermatogonia, red arrows denote STRA8-negative spermatogonia, and stages are indicated by roman numerals in the center of the tubules. Bars = 50 μm. **D**) Graphs depicts quantification of the numbers of STRA8-positive spermatogonia per tubule in four different groups of stages (XII–I, II–VI, VII–VIII, IX–XI) from vehicle control (black bars) and RA-treated (white bars) vitamin A-sufficient adult male mice. The average number (n = 3) of STRA8-positive spermatogonia per tubule is given on the Y axis with the stages listed on the X axis. The error bars represent SEM (***$P < 0.0005$, **$P < 0.01$).

testes. This observation was supported by the lack of germ cells containing detectable STRA8 protein (Fig. 6B) in the WIN 18,446-treated testes. Following injection, RA levels within the vehicle control-treated testes first increased, possibly due to an increase in the number of preleptotene spermatocytes within these testes, and then decreased over the treatment window (Fig. 6A), likely the result of increasing numbers of pachytene spermatocytes as the testis develops and, as a result, dilution of RA levels. In contrast, RA levels were found to cycle in the WIN 18,446/RA-treated animals (Fig. 6A). RA levels peaked significantly at 1, 6–8, and 14–16 days postinjection in the WIN 18,446/RA-treated animals, whereas RA levels in the testis at 4 and 12 days postinjection approached those detected in the zero time samples (Fig. 6A). Immunohistochemical analysis revealed that the time points displaying peaks in RA concentration corresponded with testes exhibiting STRA8-positive spermatogonia, STRA8-positive preleptotene spermatocytes, or both (Fig. 6, C and E), whereas STRA8 could not be detected within testes containing very little RA (Fig. 6, A and D).

RA Levels Are Highest at Stage VIII–XI of the Seminiferous Epithelial Cycle

A pulse of RA coinciding with Stages VIII and XI was also detected in the synchronized adult testis (Fig. 7). Following WIN 18,446/RA treatment, male mice were left to recover for between 42 and 50 days postinjection, and RA levels were measured within testis samples that were collected at 12 h intervals during this recovery window. These levels were then graphed according to the midpoint of synchrony for each sample, representative of progression through the cycle of the seminiferous epithelium [24, 25]. No variations in RA levels were detected in vehicle control samples collected across the same recovery window (Fig. 7). However, a pulse of RA was present within the WIN 18,446/RA-treated adult testis samples, with the highest concentrations of RA measured in testes

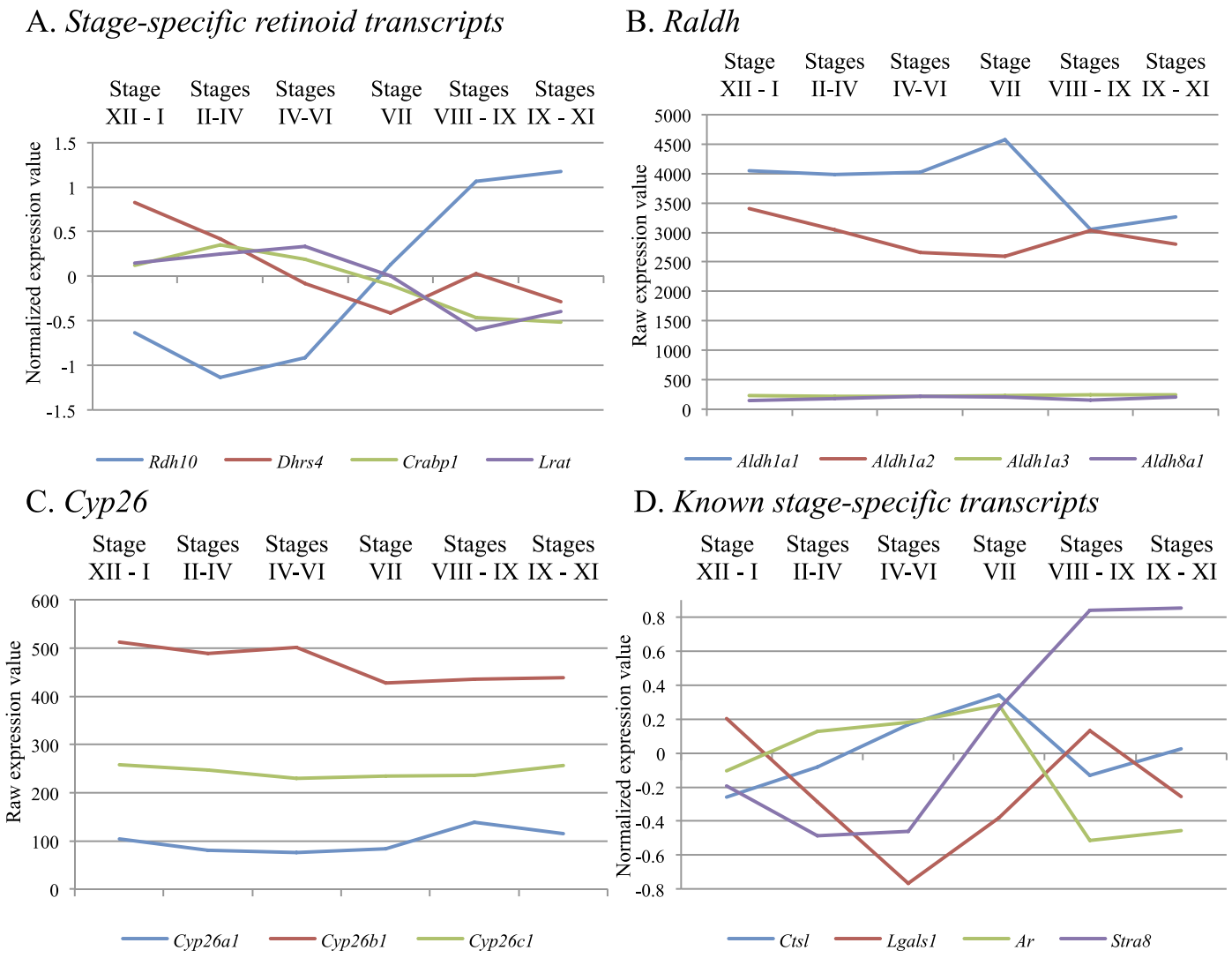

FIG. 5. Cyclic changes in retinoid metabolizing enzymes can be detected in the synchronized testis. Graphs depicting either normalized (**A** and **D**) or raw (**B** and **C**) microarray expression data for various retinoid storage, binding, and metabolism genes and transcripts known to exhibit stage-specificity in adult mouse testes displaying synchronized spermatogenesis. Retinoid-related transcripts demonstrating statistically significant stage-specificity are shown in **A**, the absence of stage-specificity for the RALDH and CYP26 enzymes can be seen in **B** and **C**, respectively, and the validity of the microarray is shown in **D**, which depicts expression of known stage-specific transcripts consistent with previous publications [17, 20, 28, 29]. For each graph, the Y axis displays the microarray expression value with the stage(s) of the seminiferous epithelium given on the X axis. The normalized expression value was plotted for two of these graphs (**A** and **D**) to aid in visualizing transcripts that have very different raw expression values but display interesting trends in expression across the cycle.

synchronized at Stages VIII and IX of the cycle, and the lowest levels detected during Stages II–VI (Fig. 7). Window width analysis revealed that as the percentage of Stage VI and VII dropped within samples, RA levels increased, however as the percentage of Stage VIII and IX dropped within samples, so too did the RA concentration (horizontal black error bars in Fig. 7).

DISCUSSION

This study represents the first quantification of a RA gradient formed with testis tubules and indicates that this gradient is the trigger for the cycle of the seminiferous epithelium. Until now, changing levels of RA along the length of a testis tubule could only be hypothesized via interpretation of mRNA and protein localization studies. Via the use of our novel WIN 18,446/RA spermatogenic synchrony protocol and a highly sensitive quantitative assay, we, for the first time, have shown that processive pulses of RA are present in a stage-specific manner and align with the tubules that contain the spermatogonia/spermatocyte association characteristic of Stages VIII–IX in the adult testis.

This study also represents the first complete stage-specific localization pattern for STRA8 in the adult mouse testis. STRA8 displayed both stage- and intracellular-specific staining, with the protein detected in spermatogonia from Stages VIII–III, but switching from being present in both the nucleus and cytoplasm to predominantly nuclear across these stages as well as in preleptotene and leptotene spermatocytes at Stages VIII–X. This pattern in the wild-type adult testis does differ slightly with a recently published review that depicted STRA8 as being present in preleptotene spermatocytes at both Stage VII and VIII and only in spermatogonia until Stage I [18]. These discrepancies are likely the result of differences in testis fixation procedures, antigen recognition, and histological interpretation of the stages based on the visualization technique

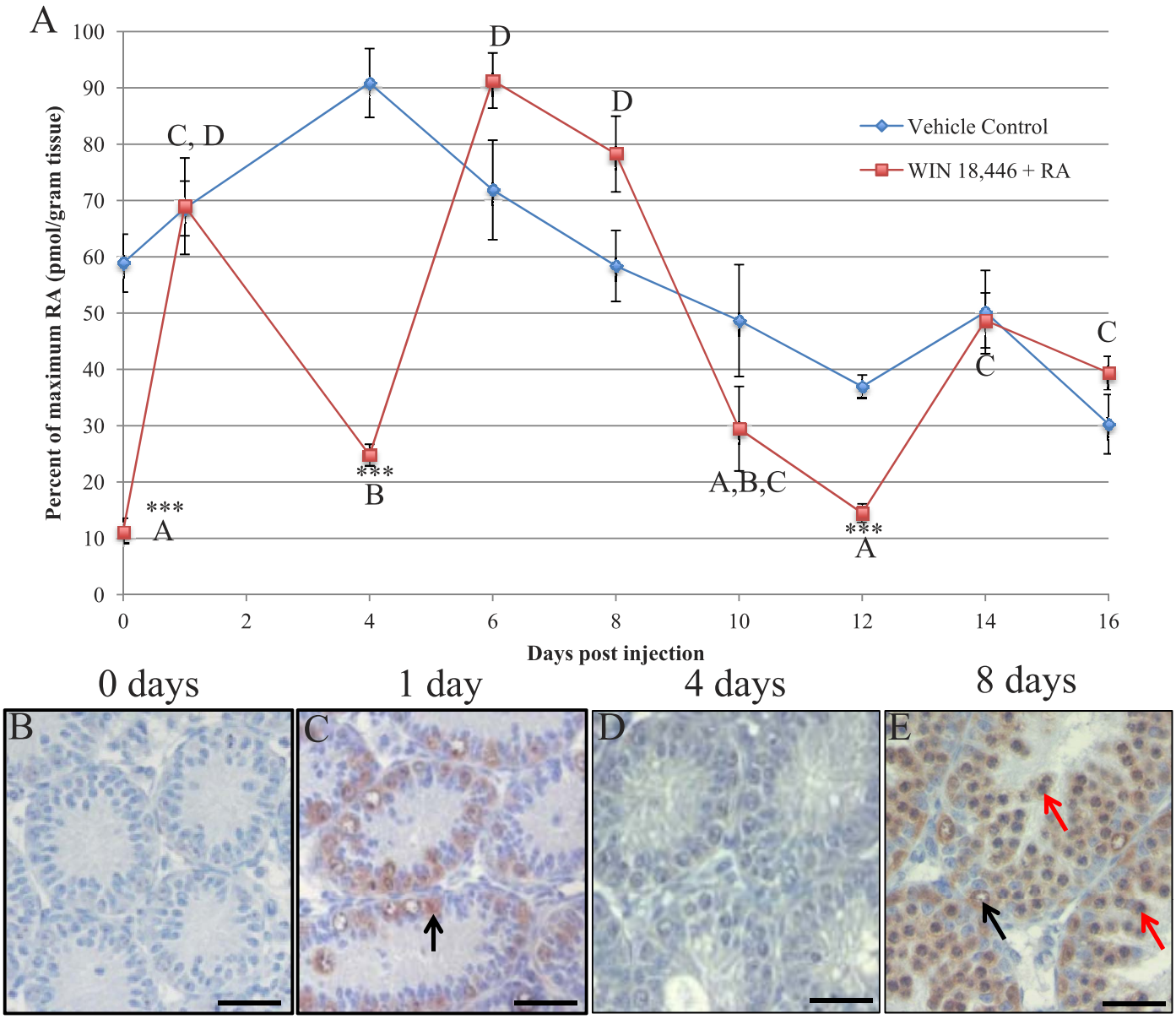

FIG. 6. Pulses of RA can be detected in the synchronized neonatal testis. **A**) Graph depicts RA levels in vehicle control (blue line) and WIN 18,446/RA-treated testes (red line) over the course of the first two waves of synchronized spermatogenesis. The treated animals received either an injection of vehicle control (control samples) or RA (WIN 18,446/RA-treated samples) at time zero. Percent of maximum RA level is given on the Y axis and has been plotted against days postinjection on the X axis. Student *t*-tests were performed to compare treated to vehicle control samples at each time point (asterisks) and to compare only the treated samples between time points (letters). Asterisks (***) denote a significant difference ($P < 0.001$) between treated and vehicle control samples. Time points marked with different letters indicated statistically different ($P < 0.05$) RA levels between samples from the WIN 18,446/RA-treated animals. **B**–**E**). Pictures depicting STRA8 localization in cross-sections of testes collected from WIN 18,446 only-treated animals (**B**) and from animals allowed either 1 day (**C**), 4 days (**D**), or 8 days (**E**) of recovery following WIN 18,446/RA treatment. Black arrows denote STRA8-positive spermatogonia, and red arrows denote STRA8-positive preleptotene spermatocytes. Bars = 20 μm.

utilized. However, it is clear from this study and previous publications that STRA8 is expressed in a tubule- and stage-specific manner throughout the development of the postnatal testis, and these data suggest that RA is only present in specific segments of testis tubules.

Limited RA availability during specific stages within the testis is also supported by our observation that significantly more STRA8-positive spermatogonia were present in Stages II–VII following a single injection of RA. Based on this, it is highly likely that induced changes to testicular RA levels will drastically alter STRA8 localization patterns. This has been observed in testes following the disruption of RA synthesis [22, 30], and a previous publication reported that exposure of the testis to exogenous RA for 24 h could induce STRA8 expression in spermatogonia in other than Stages VI–VIII [20]. These data imply that Stages II–VII are vulnerable to changes in retinoid levels within the testis, and presumably, treatment with exogenous RA was able to override the mechanism usually in place to limit RA availability within these stages. As a result, spermatogonia were exposed to RA and were able to express STRA8 in response, when under normal conditions this exposure would not have occurred. These observations also provide support for the hypothesis that the undifferentiated spermatogonia present within Stages II–VII have acquired the ability to respond to RA and RA

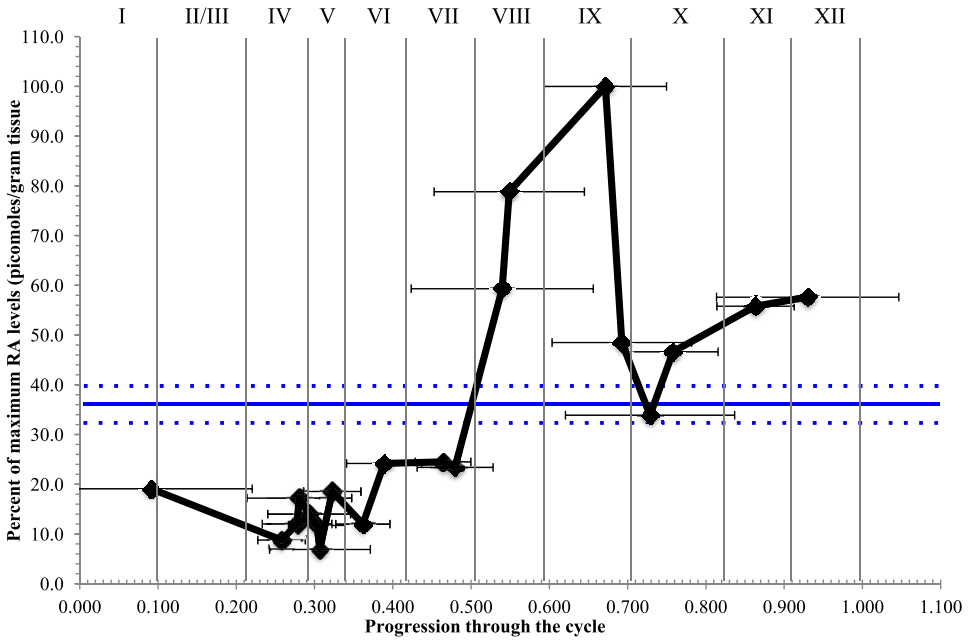

FIG. 7. RA concentration peaks at Stage IX of the cycle of the seminiferous epithelium. Graph depicts RA levels in adult mouse testes treated with either vehicle control (blue line) or WIN 18,446 and RA (black line) to synchronize spermatogenesis. Samples (n = 20) from the WIN 18,446/RA-treated animals were collected at 12 h intervals between 42 and 50 days postinjection and plotted according to their midpoint of synchrony, which is representative of progression through the spermatogenic cycle (X axis). RA concentration is given as a percentage of the maximum level detected (pmol/g tissue weight) and is given on the Y axis. Student *t*-tests were performed and demonstrated that there is significantly higher RA levels in Stages VII–IX ($P < 0.05$) and that there is significantly lower RA levels in Stages II–VI ($P < 0.001$) when compared to all the other stages. Samples (n = 5) from the vehicle control-treated animals were collected at 2 day intervals between 42 and 50 days postinjection. The average RA concentration (given as percentage of the maximum level detected) measured in the vehicle control samples is represented by the solid blue line, with the dotted line above and below representing the SEM, because progression through the cycle cannot be calculated for nonsynchronized samples. The black horizontal error bars represent the window width analysis for the WIN 18,446/RA samples.

availability is the limiting factor regarding when these spermatogonia differentiate.

To date, the majority of support for a pulse of RA being produced within the seminiferous epithelium at Stage VIII of the cycle has been derived from qualitative mRNA and/or protein localization studies that have suggested that: 1) RA exposure is limited during Stages I–VI, just before spermatogonial differentiation and meiotic onset, as RA storage is promoted, 2) RA synthesis via the RALDH enzymes occurs during Stages VII–XII, and 3) RA degradation by the CYP26 enzymes appears to be promoted after spermatogonial differentiation has taken place, in Stages VIII–XI [16, 17]. While these in situ hybridization and immunohistochemistry studies have been very useful in determining which testicular cell types contain retinoid-metabolizing mRNAs and proteins, no quantitative conclusions regarding expression levels can be drawn from these studies. The microarray analysis presented here supports the hypothesis that retinoid storage is promoted during Stages I–VI but, in contrast to the published studies, suggests that no variations in the levels of either RALDH or CYP26 enzymes exist across the cycle. This discrepancy is likely the result of the qualitative nature of mRNA or protein localization studies and the strength of the WIN 18,446/RA synchronization method to enable stage-specific transcript analysis. Instead, this analysis implies that perhaps the RDH and DHRS enzymes and the RA binding proteins are potential candidates for contributing to how RA levels are regulated in a pulsatile manner along testis tubules. RA synthesis from retinol is a two-step process with the intermediate product, retinaldehyde, generated by a reversible reaction catalyzed by either the RDH or DHRS enzymes. In addition, the CRABP proteins act to chaperone RA within cells, with CRABP1 thought to predominantly shuttle RA toward the CYP26 enzymes rather than target it for binding to RA receptors [9]. *Rdh10, Dhrs4, Crabp1,* and *Lrat* were all expressed in a stage-specific manner, so it is plausible that in addition to retinoid storage, the retinol to retinaldehyde conversion and the shuttling of RA within cells could contribute significantly to how RA levels are regulated within the seminiferous epithelium. The next steps will be to generate conditional knockout models to determine whether the coordination of oxidase/reductase activity occurs in a cell-specific manner and provides retinaldehyde only at specific points along testis tubules.

The identification of significant stage-specific expression patterns for RDH or DHRS enzymes across the cycle is novel and consistent with similar data recently generated by studies of RA biosynthesis in cell lines and the mammalian embryo. RDH10 and DHRS3 mutually activate one another and, as a result, carefully balance the production of retinaldehyde versus retinol [31]. Examination of embryos carrying point mutations or global deletions of either *Rdh10* or *Dhrs3* revealed severe developmental defects occur in the absence of either enzyme and demonstrate that both are critical for normal development [32, 33]. The essential role of the RALDH enzymes during embryogenesis has been well studied (reviewed in [34]), and collectively, these data suggest that the spatiotemporal control of RA biosynthesis can be tightly regulated at both steps in the oxidation process. The microarray data we present here also support this conclusion and suggest, for the first time, that the spatiotemporal regulation of RA biosynthesis in the postnatal testis may be predominantly regulated at the level of the reversible retinol to retinaldehyde step.

Due to the complexity and heterogeneity of the wild-type testis, measuring RA levels across the cycle of the seminiferous

epithelium in a wild-type testis has been technically challenging. Quantification of molecules within either individual cell types or single stages in a wild-type testis is impossible without physical separation and/or isolation of the cells or tubule segments of interest. Given that RA is a highly light-sensitive molecule (extensive degradation and isomerization occurs within 10–30 min under fluorescent lights) and present within the testis at pmol/gram of tissue [35], it is highly likely that RA measurements made within isolated cells or tubule segments will not be accurate due to degradation or inadequate amounts of cells/tissue. Our WIN 18,446/RA protocol enabled us to circumvent these issues and quantify RA levels at specific stages during male germ cell development.

Stage VIII is of significant interest as several crucial germ cell differentiation steps take place during this stage, and RA is linked to successful completion of all of these events. In addition to its well-characterized role in driving spermatogonial differentiation [8], RA signaling is now thought to contribute to the reorganization of the blood-testis barrier [36] and the release of spermatozoa from the seminiferous epithelium [37, 38], all three of which occur during Stage VIII. Combining our WIN 18,446/RA synchrony protocol with a highly sensitive assay has allowed us to accurately measure RA levels when only one or two different types of germ cells or stages are present and confirmed that pulses of RA occur at Stage VIII–IX of the cycle of the seminiferous epithelium. These measurements, combined with our observations regarding STRA8 localization in the wild-type and vitamin A-perturbed testis, prove what has been suggested by the retinoid-metabolizing enzyme localization studies and indicate that RA morphogen gradients are present in the postnatal testis as a means of triggering the cyclic entry of spermatogonia into their differentiation pathway. These RA gradients must be processive along the tubules and are directly responsible for the cyclic nature and continuous sperm production characteristic of mammalian males.

ACKNOWLEDGMENT

We would like to acknowledge the assistance of Derek Pouchnik and the Laboratory for Biotechnology and Bioanalysis at Washington State University for assistance with the microarray analysis.

REFERENCES

1. Begemann G, Meyer A. Hindbrain patterning revisited: timing and effects of retinoic acid signalling. Bioessays 2001; 23:981–986.
2. Briggs LJ, Stein D, Goltz J, Corrigan VC, Efthymiadis A, Hubner S, Jans DA. The cAMP-dependent protein kinase site (Ser312) enhances dorsal nuclear import through facilitating nuclear localization sequence/importin interaction. J Biol Chem 1998; 273:22745–22752.
3. Diez del Corral R, Olivera-Martinez I, Goriely A, Gale E, Maden M, Storey K. Opposing FGF and retinoid pathways control ventral neural pattern, neuronal differentiation, and segmentation during body axis extension. Neuron 2003; 40:65–79.
4. Towers M, Wolpert L, Tickle C. Gradients of signalling in the developing limb. Curr Opin Cell Biol 2012; 24:181–187.
5. Bowles J, Knight D, Smith C, Wilhelm D, Richman J, Mamiya S, Yashiro K, Chawengsaksophak K, Wilson MJ, Rossant J, Hamada H, Koopman P. Retinoid signaling determines germ cell fate in mice. Science 2006; 312: 596–600.
6. Koubova J, Menke DB, Zhou Q, Capel B, Griswold MD, Page DC. Retinoic acid regulates sex-specific timing of meiotic initiation in mice. Proc Natl Acad Sci U S A 2006; 103:2474–2479.
7. Shimozono S, Iimura T, Kitaguchi T, Higashijima S, Miyawaki A. Visualization of an endogenous retinoic acid gradient across embryonic development. Nature 2013; 496:363–366.
8. Hogarth CA, Griswold MD. The key role of vitamin A in spermatogenesis. J Clin Invest 2010; 120:956–962.
9. Napoli JL. Physiological insights into all-trans-retinoic acid biosynthesis. Biochim Biophys Acta 2012; 1821:152–167.
10. Kane MA, Folias AE, Wang C, Napoli JL. Ethanol elevates physiological all-trans-retinoic acid levels in select loci through altering retinoid metabolism in multiple loci: a potential mechanism of ethanol toxicity. FASEB J 2010; 24:823–832.
11. Kane MA, Folias AE, Wang C, Napoli JL. Quantitative profiling of endogenous retinoic acid in vivo and in vitro by tandem mass spectrometry. Anal Chem 2008; 80:1702–1708.
12. Chung SS, Wolgemuth DJ. Role of retinoid signaling in the regulation of spermatogenesis. Cytogenet Genome Res 2004; 105:189–202.
13. Bonet ML, Ribot J, Palou A. Lipid metabolism in mammalian tissues and its control by retinoic acid. Biochim Biophys Acta 2012; 1821:177–189.
14. Duester G. Retinoic acid synthesis and signaling during early organogenesis. Cell 2008; 134:921–931.
15. Hogarth CA, Amory JK, Griswold MD. Inhibiting vitamin A metabolism as an approach to male contraception. Trends Endocrinol Metab 2011; 22: 136–144.
16. Vernet N, Dennefeld C, Rochette-Egly C, Oulad-Abdelghani M, Chambon P, Ghyselinck NB, Mark M. Retinoic acid metabolism and signaling pathways in the adult and developing mouse testis. Endocrinology 2006; 147:96–110.
17. Sugimoto R, Nabeshima Y, Yoshida S. Retinoic acid metabolism links the periodical differentiation of germ cells with the cycle of Sertoli cells in mouse seminiferous epithelium. Mech Dev 2012; 128:610–624.
18. Mark M, Teletin M, Vernet N, Ghyselinck NB. Role of retinoic acid receptor (RAR) signaling in post-natal male germ cell differentiation. Biochim Biophys Acta (in press). Published online ahead of print 27 May 2014; DOI: 10.1016/j.bbagrm.2014.05.019
19. Snyder EM, Small C, Griswold MD. Retinoic acid availability drives the asynchronous initiation of spermatogonial differentiation in the mouse. Biol Reprod 2010; 83:783–790.
20. Zhou Q, Nie R, Li Y, Friel P, Mitchell D, Hess RA, Small C, Griswold MD. Expression of stimulated by retinoic acid gene 8 (Stra8) in spermatogenic cells induced by retinoic acid: an in vivo study in vitamin A-sufficient postnatal murine testes. Biol Reprod 2008; 79:35–42.
21. Russell LD, Ettlin RA, Sinha Hikim AD, Clegg EP. Histological and Histopathological Evaluation of the Testis. St. Louis, MO: Cache River Press; 1990.
22. Hogarth CA, Evanoff R, Mitchell D, Kent T, Small C, Amory JK, Griswold MD. Turning a spermatogenic wave into a tsunami: synchronizing murine spermatogenesis using WIN 18,446. Biol Reprod 2013; 88: 40.
23. Paik J, Haenisch M, Muller CH, Goldstein AS, Arnold S, Isoherranen N, Brabb T, Treuting PM, Amory JK. Inhibition of retinoic acid biosynthesis by the bisdichloroacetyldiamine WIN 18,446 markedly suppresses spermatogenesis and alters retinoid metabolism in mice. J Biol Chem 2014; 289:15104–15117.
24. van Beek ME, Meistrich ML. Stage-synchronized seminiferous epithelium in rats after manipulation of retinol levels. Biol Reprod 1991; 45:235–244.
25. Siiteri JE, Karl AF, Linder CC, Griswold MD. Testicular synchrony: evaluation and analysis of different protocols. Biol Reprod 1992; 46: 284–289.
26. Loveland KL, Hogarth C, Szczepny A, Prabhu SM, Jans DA. Expression of nuclear transport importins beta 1 and beta 3 is regulated during rodent spermatogenesis. Biol Reprod 2006; 74:67–74.
27. Arnold SL, Amory JK, Walsh TJ, Isoherranen N. A sensitive and specific method for measurement of multiple retinoids in human serum with UHPLC-MS/MS. J Lipid Res 2012; 53:587–598.
28. Johnston DS, Wright WW, Dicandeloro P, Wilson E, Kopf GS, Jelinsky SA. Stage-specific gene expression is a fundamental characteristic of rat spermatogenic cells and Sertoli cells. Proc Natl Acad Sci U S A 2008; 105: 8315–8320.
29. Linder CC, Heckert LL, Roberts KP, Kim KH, Griswold MD. Expression of receptors during the cycle of the seminiferous epithelium. Ann N Y Acad Sci 1991; 637:313–321.
30. Li H, Palczewski K, Baehr W, Clagett-Dame M. Vitamin A deficiency results in meiotic failure and accumulation of undifferentiated spermatogonia in prepubertal mouse testis. Biol Reprod 2011; 84:336–341.
31. Adams MK, Belyaeva OV, Wu L, Kedishvili NY. The retinaldehyde reductase activity of DHRS3 is reciprocally activated by retinol dehydrogenase 10 to control retinoid homeostasis. J Biol Chem 2014; 289:14868–14880.
32. Sandell LL, Sanderson BW, Moiseyev G, Johnson T, Mushegian A, Young K, Rey JP, Ma JX, Staehling-Hampton K, Trainor PA. RDH10 is essential for synthesis of embryonic retinoic acid and is required for limb, craniofacial, and organ development. Genes Dev 2007; 21:1113–1124.
33. Rhinn M, Schuhbaur B, Niederreither K, Dolle P. Involvement of retinol dehydrogenase 10 in embryonic patterning and rescue of its loss of

function by maternal retinaldehyde treatment. Proc Natl Acad Sci U S A 2011; 108:16687–16692.
34. Kumar S, Sandell LL, Trainor PA, Koentgen F, Duester G. Alcohol and aldehyde dehydrogenases: retinoid metabolic effects in mouse knockout models. Biochim Biophys Acta 2012; 1821:198–205.
35. Kane MA, Chen N, Sparks S, Napoli JL. Quantification of endogenous retinoic acid in limited biological samples by LC/MS/MS. Biochem J 2005; 388:363–369.
36. Hasegawa K, Saga Y. Retinoic acid signaling in Sertoli cells regulates organization of the blood-testis barrier through cyclical changes in gene expression. Development 2012; 139:4347–4355.
37. Vernet N, Dennefeld C, Klopfenstein M, Ruiz A, Bok D, Ghyselinck NB, Mark M. Retinoid X receptor beta (RXRB) expression in Sertoli cells controls cholesterol homeostasis and spermiation. Reproduction 2008; 136:619–626.
38. Vernet N, Dennefeld C, Guillou F, Chambon P, Ghyselinck NB, Mark M. Prepubertal testis development relies on retinoic acid but not rexinoid receptors in Sertoli cells. EMBO J 2006; 25:5816–5825.